Thermal Stability Testing of Two-Phase Thermal Control Hardware for the Surface Water Ocean Topography Mission

Ruwan P. Somawardhana[1]
Jet Propulsion Laboratory/California Institute of Technology, Pasadena, CA, 91109

The thermal architecture for the Surface Water Ocean Topography mission utilizes loop heat pipes and constant conductance heat pipes to transport waste heat (> 1000 Watts) from the instrument electronics to the radiator. The main thermal design risk is the ability to maintain a temporal stability of <0.05 Celsius per minute in a low earth orbit environment. The stringent thermal requirements are part of the overall error budget needed to meet the primary mission science objectives. A testbed was developed to simulate flight-like loads and environments in order to validate the thermal subsystem can meet the temporal stability requirements. Preliminary testing showed that the thermal control system can meet the stability requirement and that loop heat pipes are actually helping to maintain stability during transient sink temperature changes for this specific flight application and boundary conditions.

Nomenclature

°C	=	Degrees Celsius
CCHP	=	Constant Conductance Heat Pipe
CNES	=	French National Space Studies Center
ERBE	=	Earth Radiation Budget Experiment
KaRIn	=	Ka-band Radar Interferometer
LHP	=	Loop Heat Pipe
min	=	minute
NASA	=	National Aeronautics and Space Administration
PRT	=	Platinum Resistance Thermometer
SWOT	=	Surface Water Ocean Topography
TCS	=	Thermal Control System
W	=	Watt

I. Introduction

THE Surface Water Ocean Topography (SWOT) mission is a joint project between National Aeronautics and Space Administration (NASA) and French National Space Studies Center (CNES) with a planned launch in 2020. The primary science goal is to measure ocean circulation and land hydrology to a spatial resolution of 15 to 200 km. This would help fill a data gap that currently exists between in-situ based measurements and current airborne and space based measurements. The data will help scientists better characterize the global continental surface water inventory (lakes, reservoirs, wetlands, and large rivers) as well as supplement oceanic circulation measurements at scales currently not available. This additional data can ultimately aid climate modeling.

The SWOT mission is composed of six payloads that include an altimeter, microwave radiometer, global positioning systems, a laser retroreflector, and an interferometer. The primary instrument is the Ka-band Radar Interferometer (KaRIn) which will make large swath measurements to measure the surface elevations of water bodies. The precision measurements needed to meet the primary science objectives impose challenging requirements for the engineering team to accommodate for the KaRIn instrument design. One of the main thermal challenges is to maintain precise temporal stability requirements (<0.05 °C/min) in a low earth orbit while managing large electronic dissipation (>1000 W) that configurationally requires co-location.

[1]SWOT Payload Thermal Systems Lead, Instrument and Payload Thermal Engineering, 4800 Oak Grove Dr. M/S 125-123, Pasadena, CA 91109.

II. KaRIn Thermal Design and Validation Approach

A. Thermal Architecture

The KaRIn instrument has many design challenges across subsystems including the electronics, structural, and thermal subsystems. All of these challenges have interdependencies between subsystems and therefore requires success in all areas in order to meet the overall performance criteria. In order to reduce signal noise within the electronic subsystem, the thermal stability of the electronics is a key and driving thermal requirement. The required stability for the electronics is <0.05 °C/min over a timescale of 2.6 minutes. The timescale relates to the time it takes for KaRIn to map ocean height measurements at the scale of 1,000 km per the planned SWOT orbit.

As discussed in detail by R. Somawardhana[1], in order to meet the spatial design constraints and high electronics waste dissipation (>1,000 W), the thermal architecture consists of four zones. Each zone is comprised of a thermal pallet with three to five embedded constant conductance heat pipes (CCHPs) and one loop heat pipe (LHP) as depicted in Figure 1, hereby referred to as the thermal control system (TCS). While the use of LHPs solved the heat transport, limited survival power, flight system integration, and ground testing problems, they introduce a concern regarding thermal stability. Depending on the LHP boundary conditions, high frequency and low frequency oscillations have been observed as discussed by J. Ku[2,3]. These oscillations can be driven by improper radiator sizing, heat source fluctuations, thermal mass, and varying heat sinks.

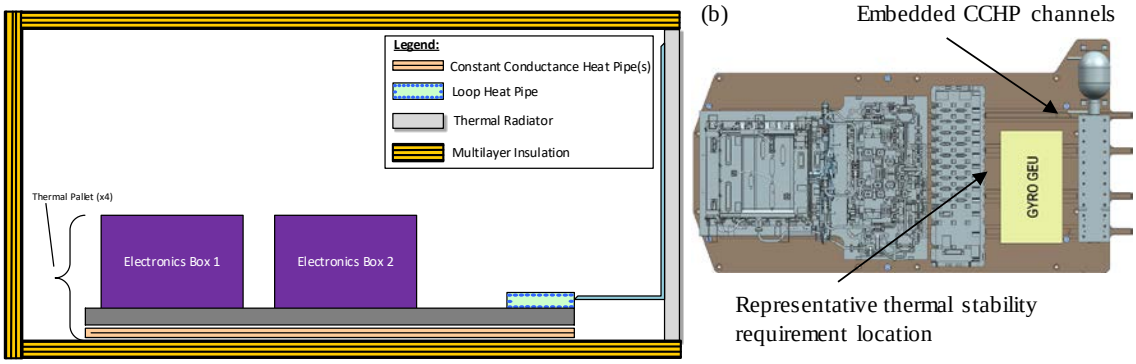

Figure 1. (a) KaRIn system-level block diagram[1]. (b) Flight layout of thermal pallet zone.

B. Validation Approach

To protect against improper radiator sizing, requirements were generated to clearly define the minimum and maximum thermal dissipation per zone allowed and additional margin has been held to capture any unknown variability. With the ability to conservatively size the radiator, radiator sizing impact is low risk and bounds the maximum thermal dissipation requirement. The thermal dissipation of the electronics is stable by design (<0.051% variability) and therefore are not a source of thermal instability.

The main stability concern remaining with the LHP application is assessing the impact of a varying heat sink. Initial design assessments showed the system thermal mass was sufficient to meet the stability requirements. All stability assessments are made with the lowest estimated subsystem mass for conservatism. For the initial assessment, the thermal model used an overall conductance of the LHP between the evaporator and condenser based on steady-state LHP test results from previous programs. Lack of modeling the two-phase physics, especially for a transient condition, is a known simplification and limitation. As the instrument design matured and higher fidelity system-level models were built (but using the same simplification for the LHP modeling), reassessment showed a non-compliance to meeting the stability requirement as shown in Table 1. It was presumed that the lack of fidelity in the modeling of the LHP could be a factor in making this assessment overly conservative.

Table 1. Preliminary design thermal model predictions

Pallet	Max Drift Rate [°C/min]	Violation Duration [min]
RFU	0.03	none
KDES	0.06	14
EIK	0.07	21
HVPS	0.03	none

Due to the difficulty of accurately modeling transient behavior of LHPs, the primary design validation and requirement verification method was determined to be via testing. The test campaign consisted of two primary phases, or 'Steps'. Step 1 was a fact-finding process to gain familiarity with the hardware and scope the design of the testbed[1]. Step 2 is a fight-like configuration that is planned to verify requirements, discussed in Section III. Step 3 is a contingency configuration in the event that thermal vacuum testing is required due to ambient testing limitations.

With thermal stability being a key and driving requirement, the project agreed early-on to maintain a spacecraft attitude which minimized the KaRIn radiators solar view factor with a maximum solar view angle of 4.5°. With this guaranteed attitude, the primary thermal disturbance results from albedo and Earth IR. The overall worst case sink temperature fluctuation was determined to be 8°C/min over a three-minute period from the Earth Radiation Budget Experiment (ERBE) datasets[1]. This three-minute duration aligns well with the stability requirement timescale of 2.6 minutes. While this is coincidental, it does help support the validity of using the ERBE dataset due to the similar orbital period (96 min vs 103 min).

III. Testbed

A. Testbed Design

In order to achieve the highest fidelity testbed and capture any second order effect, significant effort was made to have as close to a flight representation of the system as possible given the best available design information at the time. This included flight-like TCS hardware and mass models.

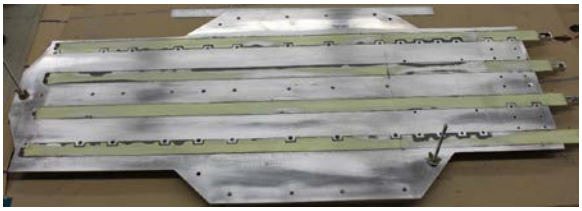

Figure 3. Thermal pallet post integration of CCHPs

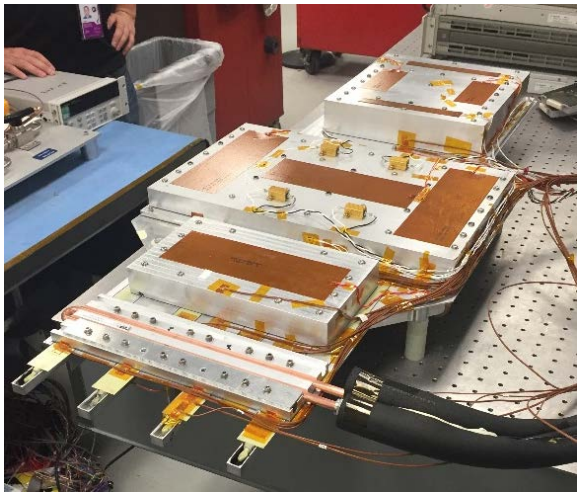

Figure 2. Fully integrated and instrumented testbed thermal pallet.

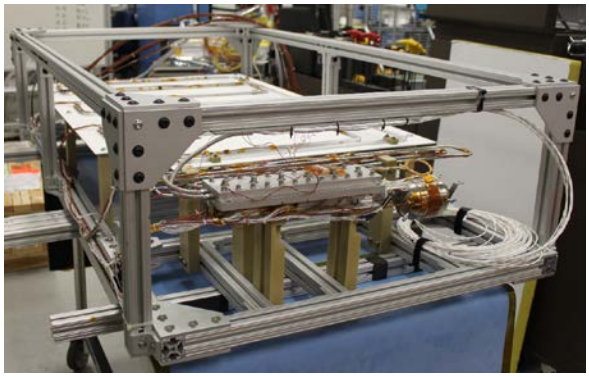

Figure 4. LHP with painted radiator (top surface in figure) and instrumentation.

The thermal pallet consisted of a hogged out aluminum structure that had four CCHPs embedded in channels via epoxy (Figure 3). The CCHPs were procured to flight quality standards and the thermal pallet was designed to match the flight design at the time of manufacture. The integration used epoxy planned for the final flight application. Thermal masses and heaters were then added to represent the electronics boxes. Effort was made to distribute the mass and power to represent the flight configuration. The final integrated thermal pallet is shown in Figure 2.

A LHP (Figure 4) was procured to the flight system specifications known at the time of procurement. Table 2 compares the testbed LHP design parameters to the current flight parameters. The procured LHP was designed to specifically have a low heat transfer between the reservoir and liquid return line. This design choice was made in an effort to provide dampening between the condenser and the evaporator which would aid in meeting the driving stability requirement as well as reduces heat leaks between the reservoir and liquid line.

While the Step 1 testing configuration had a conductive interface between the sink temperature source and LHP evaporator[1], it was determined that this setup was not appropriate. The high conductance of a conductive interface with respect to the flight radiative interface required the sink temperature to be set warmer as well as have a lower rate of change in order to mimic the flight environment. In order to eliminate these variables while not having an overly conservative test (using a conductive interface without modifying the sink temperature and/or rate of change), it was decided that the Step 2 configuration be designed with a radiative approach. Once the LHP was received, the radiator was painted with flight quality materials and a custom heat sink was integrated. The heat sink consisted of an aluminum plate instrumented with heaters and bolted to a heat exchanger that was cooled via an external fluid chiller (Figure 5). The heat sink was coupled to the radiator via radiation, gas conduction and natural

Table 2. Comparison of testbed LHP design parameters against flight design best estimate.

Design	Step 2 (Phase A)	Flight (Phase B)
Working Fluid	Propylene	Propylene
Max transport line length [m]	2	2.3
Max Cond Line Length [m]	6.9	17.9
Heat Transport Capacity Range [W]	150 to 350	211 to 370*
Thermal Conductance from Evap-to-Cond [W/°C]	30	40
Evap Operating Temperature [°C]	-10 to 40	-15 to 30

*combined range across all LHPs is 74W to 370W

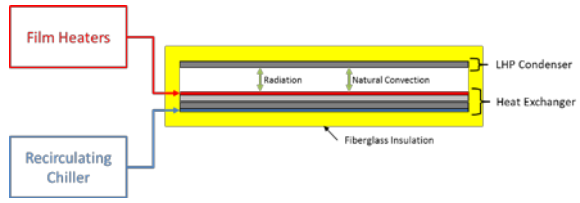

Figure 5. LHP condenser heat sink configuration.

convection. While the configuration minimized gas conduction by providing a minimum gap between the LHP condenser and heat sink and almost eliminates natural convection due to spatial orientation with respect to buoyancy forces, the overall coupling still had some amount of gas conduction and natural convection (estimated at < 3% of total dissipated power). This was acceptable for the purposes of the testbed due to the additional heat transfer which makes the setup conservative from a stability perspective (greater coupling of the LHP to the sink environment). This setup was also ideal for Step 3, testing in vacuum, if these additional heat loads and disturbances prevented the required stability from being achieved.

The last process was to mate the thermal pallet with the LHP and finalize the testbed integration. The entire system was well instrumented (118 measurement points) with a combination of platinum resistance thermometers (PRTs) and thermocouples. One of the primary lessons learned from Step 1 was the need for PRTs in order to obtain measurements with the desired precision[1]; PRTs were implemented in all areas deemed as critical stability measurement locations. Due to the low cost and ease of installation, thermocouples were used to compliment the PRTs for wider temperature knowledge. After the completion of instrumentation, the entire setup was insulated with a combination of multilayer insulation and fiberglass boards, and contained within a purge bag. The test article was then electrically mated to the control rack for instrumentation measurement and sink plate heater control. Finally, the recirculation bath was connected to the heat exchanger to provide the thermal sink. The entire setup is shown in Figure 6.

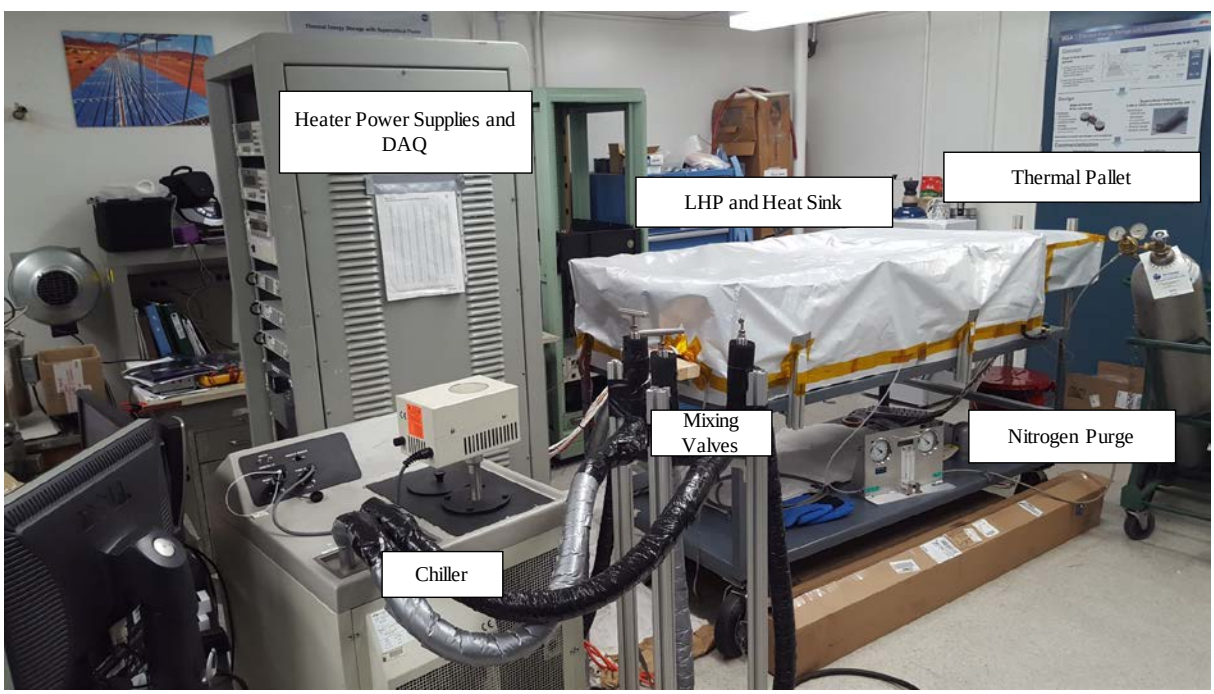

Figure 6. Fully integrated SWOT two-phase hardware thermal testbed.

B. Stability Testing and Assessment

Once fully integrated, the testbed was exercised to determine the bounds of the available capability. The initial design intent was to enable testing to bound the ERBE worst case pulses. A pulse consisting of 8 °C/min rise over three minutes followed immediately by an 8 °C/min drop over three minutes and vice versa was determined to be a

conservative approach. While the setup was able to produce a heat sink maximum cold-to-hot transient rate of 10 °C/min which exceeds the worst case expected temperature rise, it was not able to replicate the transient from hot-to-cold. Modifications to the testbed to achieve this capability are in review for future testing.

After the testbed was functionally checked out, a series of transient performance tests were performed varying the thermal pallet total dissipation as well as the heat sink temperature ramp rate. The test procedure was to operate the system such that the control point (interface of the thermal dissipation source, identified in Figure 1(b)) was at steady state with a maximum rate of change of ±0.001 °C/min. Once this steady-state was achieved, a thermal pulse was imposed on the heat sink. The primary testing focused on achieving stability with an 8 °C/min sink temperature ramp rate over a duration of 3 minutes. This was performed both at the minimum and maximum power expected during flight for the configuration tested. Table 3 shows the performance results of the primary stability tests and Figure 7 depicts the temperature profile of the system in response to the sink temperature profile. For both the low and nominal power cases, stability of < 0.05 °C/min was achieved successfully. The uncertainty on the stability is due to the partials of all of the error sources in the test setup. While this uncertainty is larger than the nominally measured value itself, even with the maximum uncertainty applied, stability was maintained with approximately a factor of two margin against the requirement. To further bound the testing, an additional test was performed by maximizing the testbed capability of sink temperature ramp rate. A sink temperature rate of change of 10 °C/min was held for approximately seven minutes. During this test, stability of 0.014 ± 0.020 °C/min was achieved, below the 0.05 °C/min requirement. It is important to point out that the stability of 0.014 °C/min was the maximum instantaneous value within the seven-minute duration and not the average stability value over the seven-minute duration which is much lower. This provided additional confidence that the system did not exhibit a performance inflection point that would be detrimental if the sink temperature rate of change happened to be larger or longer than expected.

Table 3. Stability results for heat sink transient ramp from cold-to-hot.

Test Condition	Nominal Power	Low Power
Heat Sink Start [°C]	-71.25 ± 0.75	-71.25 ± 0.75
Pallet [W]	208	75
Steady-State Pre-Ramp [°C/min]	0.000 ± 0.001	0.000 ± 0.001
Heat Sink Ramp [°C/min]	7.84 ± 0.14	7.74 ± 0.14
Pallet Stability	0.008 ± 0.020	0.000 ± 0.020

A compilation of all the stability tests performed at the nominal power of 208W is shown in Figure 8. The limited data shows stability range within 0.006 °C/min. No definitive trend was observed, partially due to the relatively high uncertainty in the measurement with respect to the target value and partially due to the small sample set (five total tests). However, it can be concluded with reasonable confidence that the system can maintain the required stability even when stacking the maximum uncertainty.

Based on the available dataset, testing showed that the system performed better than the system-level thermal model predictions as described in Section II.B. It is hypothesized that the thermal resistance between the return liquid and reservoir fluid is attenuating the overall impact of the transient environmental energy change. As the sink temperature increases, the heat transfer rate between the condenser and sink decreases. As the LHP adjusts to dissipate the full thermal load, the vapor front moves allowing for more of the condenser line length to be used at the expense of some sub-cooling, as shown in the mapped test data of Figure 9. If the return liquid were perfectly coupled to the reservoir fluid in a mass-less system, the resulting warmer return liquid would change the reservoir saturation state that, in turn, dictates the operating condition of the evaporator. However, the thermal capacitance of the reservoir mass as well as the reduced heat transfer between the return liquid and reservoir fluid dampens the LHP overall response to the sink temperature change. If the sink temperature were to stabilize at a new sink, then the TCS would eventually reach its new equilibrium. If the hypothesis with respect to the reservoir fluid-liquid return thermal coupling causing a dampening effect on the TCS to the environment is correct, then it can be extrapolated that the physics remain the same regardless of the sink temperature ramp rate direction (cold-to-hot versus hot-to-cold). While testing also showed the potential for better stability at lower heat loads as shown in the comparison in Table 3, the overlapping uncertainty in the results between low and high power modes as well as a the need for a better understanding requires further investigation before any definitive conclusion can be drawn.

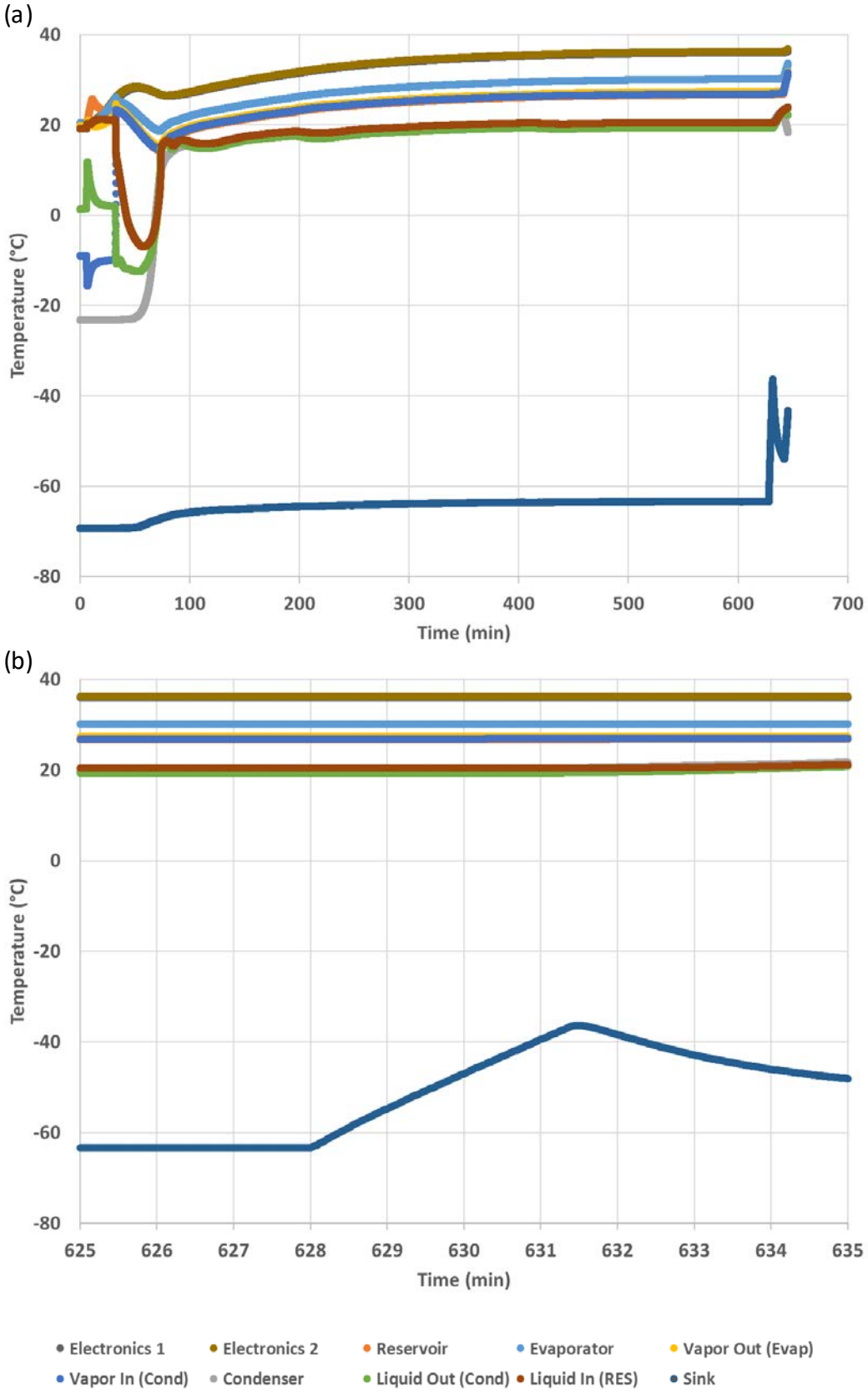

Figure 7. (a) Full test profile for nominal power case (b) profile during sink temperature ramp

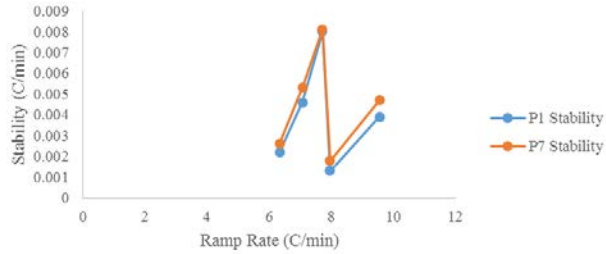

Figure 8. Measured stability (all values are ±0.02 C/min) for five different heat sink ramp rate. Thermal pallet load was 208W for all cases.

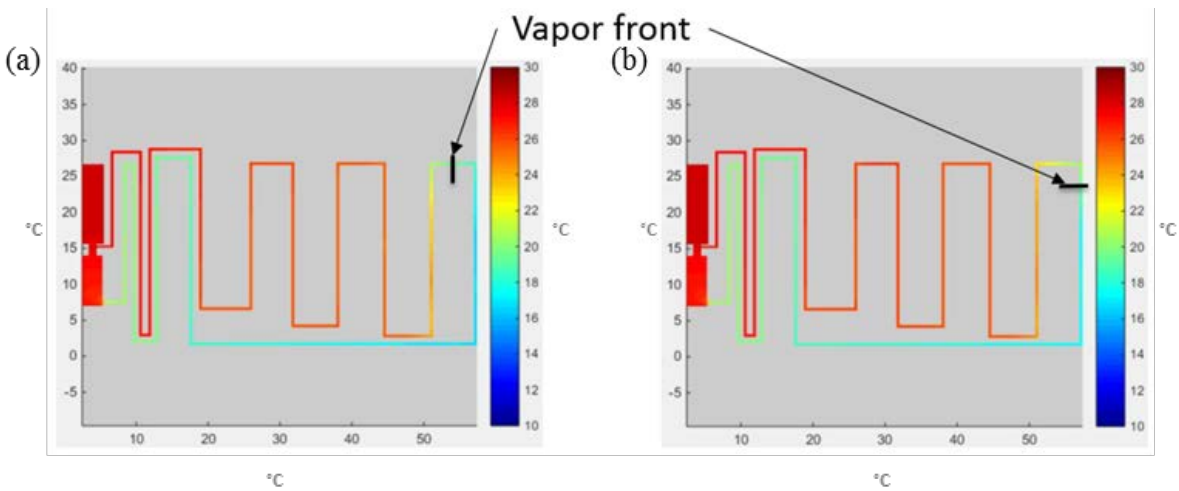

Figure 9. (a) Condenser before heat sink ramp from cold-to-hot. (b) Condenser after heat sink ramp from cold-to-hot. Note the visible movement of the vapor front within the condenser.

IV. Conclusions

The KaRIn thermal control system appears to be capable of meeting the stability requirement of < 0.05 °C/min. Testing of the full end-to-end system with a flight-like breadboard unit LHP has shown stability with almost a factor of two margin against the requirement. While testing has only been performed with a transient sink temperature change from cold-to-hot, the presumed physics should be applicable for a sink temperature change from hot-to-cold as well. It is important to validate the hypothesis with further testing before taking credit for requirement conformance but results to date look promising. Future studies would also benefit from determining the relative effect on TCS overall mass as well as dissipative power to truly understand the attenuating benefit an LHP may provide to the system.

With respect to the anticipated performance of the flight system design described in Table 2 relative to the Step 2 unit, the primary difference is condenser line length. While this is the main interface to the environment, it is anticipated that the flight design will exhibit similar stability behavior. The LHP reservoir/evaporator design of the flight unit will be the same as the Step 2 unit and therefore the thermal resistance between the liquid return and reservoir fluid will be the same which is hypothesized to be the most important design parameter with respect to thermal stability of the system. This will be formally assed by the hardware supplier during the flight design phase and then ultimately tested with the flight hardware.

Acknowledgments

The author would like to thank Eric Sunada (JPL) for the many years of mentorship and advice specifically for the SWOT Thermal subsystem design evolution as well as the implementation of the heat pipe system. Eric and Dr. Hiroki Nagai (JPL visiting professor, Tohoku University) also deserves credit for putting in the effort to help finalize the testbed setup when a dedicated test engineer was not available. Ben Furst (JPL) helped assemble and test the thermal pallet before integration to the LHP. Anthony Franklin (JPL intern, University of Michigan) deserves much

of the credit to getting the full testbed up and running and then executing the majority of the performance tests and data analysis. Raymond Higuera (JPL) and Jorge Garcia (JPL) deserve appreciation for their support and advice regarding hardware setup and integration for the testbed. Finally, special thanks go to Jentung Ku (GSFC) and Michael Nikitkin (Orbital ATK) for all of their LHP expertise and time that they have supported the SWOT Project.

The work described in this paper was carried out by the Jet Propulsion Laboratory, California Institute of Technology, under a contract with the National Aeronautics and Space Administration. Copyright 2016 California Institute of Technology. Government sponsorship acknowledged.

References herein to any specific commercial product, process, or service by trade name, trademark, manufacturer, or otherwise does not constitute or imply its endorsement by the United States Government or the Jet Propulsion Laboratory, California Institute of Technology.

References

[1]Somawardhana, R. P., "Surface Water Ocean Topography Ka-Band Radar Interferometer Payload Thermal Design Challenges," *44th International Conference on Environmental Systems*, CPICES-2014-032, pp. 2-3.

[2]Ku, J., "Low Frequency High Amplitude Temperature Oscillations in Loop Heat Pipe Operation," *SAE Technical Papers*, CP2003-01-2386, SAE International, Warrendale, 2003.

[3]Ku, J., "High Frequency Low Amplitude Temperature Oscillations in Loop Heat Pipe Operation," *SAE Technical Papers*, CP2003-01-2387, SAE International, Warrendale, 2003.